

CMS Physics Analysis Summary

Contact: cms-pag-conveners-higgs@cern.ch

2012/07/08

Search for the standard model Higgs boson decaying to tau pairs in pp collisions

The CMS Collaboration

Abstract

A search for a standard model Higgs boson decaying to tau pairs is performed using events recorded by the CMS experiment at the LHC in 2011 and 2012 at a center-of-mass energy of 7 and 8 TeV respectively. The dataset corresponds to an integrated luminosity of 10 fb^{-1} , corresponding to 4.9 fb^{-1} of data taken at 7 TeV center-of-mass energy and 5.1 fb^{-1} of data taken at 8 TeV center-of-mass energy. No excess of events is observed in the tau-pair invariant-mass spectrum. In the mass range of 110–145 GeV upper limits at 95% confidence level on the production cross section are determined. We exclude a Higgs boson with $m_H = 125 \text{ GeV}$ with a production cross section 1.06 times that predicted by the standard model.

1 Introduction

An important goal of the LHC physics program is to ascertain the mechanism of electroweak symmetry breaking, through which the W and Z bosons attain mass, while the photon remains massless. In the standard model (SM) [1–3], this is achieved via the Higgs mechanism [4–9], which also predicts the existence of a scalar Higgs boson.

Direct searches for the SM Higgs boson at the Large Electron-Positron Collider (LEP) set a limit on the mass $m_H > 114.4 \text{ GeV}$ at 95% confidence level (CL) [10]. The Tevatron collider experiments exclude the SM Higgs boson in the mass range 162 – 166 GeV [11], the ATLAS experiment in the mass range of 111.4 – 116.6 GeV , 119.4 – 122.1 GeV , and 129.2 – 541 GeV [12], and the CMS experiment in the mass range 127.5 – 600 GeV [13, 14] using the 2011 dataset. Precision electroweak data constrain the mass of the SM Higgs boson to be less than 158 GeV [15].

This Summary reports a search for the SM Higgs boson using final states with tau pairs in proton-proton collisions at $\sqrt{s} = 7$ and 8 TeV at the LHC. We use a data sample collected in 2011 and 2012 corresponding to an integrated luminosity of about 10 fb^{-1} recorded by the Compact Muon Solenoid (CMS) [16] experiment, corresponding to an integrated luminosity of 4.9 fb^{-1} of data taken at 7 TeV center-of-mass energy and 5.1 fb^{-1} of data taken at 8 TeV center-of-mass energy. Four independent tau pair final states where one or both taus decay leptonically are studied: $e\tau_h + X$, $\mu\tau_h + X$, $e\mu + X$, and $\mu\mu + X$ where we use the symbol τ_h to indicate a reconstructed hadronic decay of a tau.

The search strategy relies upon the signature of the tau pair. In order to improve the tau pair mass resolution, and to enhance the signal contribution, the selected tau pair events are classified using the signature of the production mechanism and by the transverse momentum of the reconstructed tau decay. The gluon-fusion production mechanism [17] has the largest cross section followed by vector boson fusion (VBF). The latter production mechanism is targeted by requiring two jets with a large rapidity separation [18]. Events with zero or one jet are further classified by the tau transverse momentum. The distinct topologies greatly reduce the background contribution. Additionally, Higgs boson signal events produced with a significant transverse momentum [19] benefit from a better mass resolution.

2 Trigger and event selection

The analysis makes use of the four independent tau-pair final states, $e\tau_h + X$, $\mu\tau_h + X$, $e\mu + X$, and $\mu\mu + X$. In all four channels, the reducible and irreducible backgrounds are substantial.

The trigger selection requires a combination of electron, muon and tau trigger objects [20–22]. The identification criteria and transverse momentum thresholds of these objects were progressively tightened as the LHC instantaneous luminosity increased over the data-taking period.

A particle-flow algorithm [23–25] is used to combine information from all CMS subdetectors to identify and reconstruct individual particles in the event, namely muons, electrons, photons, and charged and neutral hadrons. From the resulting particle list we reconstruct jets, hadronically-decaying taus, and missing transverse energy (E_T^{miss}), defined as the magnitude of the vector sum of the transverse momenta. The jets are reconstructed using the anti- k_T jet algorithm [26, 27] with a distance parameter of $R = 0.5$. Hadronically-decaying taus are reconstructed and identified using the hadron plus strips (HPS) algorithm, which considers candidates with one charged pion and up to two neutral pions or three charged pions [28].

For the $e\tau_h + X$ and $\mu\tau_h + X$ final state, in the region $|\eta| < 2.1$, we select events with an electron

of $p_T > 20 \text{ GeV}$ or a muon of $p_T > 17 \text{ GeV}$, together with an oppositely charged τ_h of $p_T > 20 \text{ GeV}$ within the range $|\eta| < 2.3$. The thresholds have been increased to 24 GeV and 20 GeV , respectively, in the 2012 dataset to account for higher trigger thresholds. For the $e\mu + X$ final state, we select events with an electron of $|\eta| < 2.3$ and an oppositely charged muon of $|\eta| < 2.1$, requiring $p_T > 20 \text{ GeV}$ for the highest- p_T lepton and $p_T > 10 \text{ GeV}$ for the second-highest- p_T lepton. For the $e\tau_h + X$ and $\mu\tau_h + X$ final state, we reject events with more than one electron or more than one muon of $p_T > 15 \text{ GeV}$.

Taus from Higgs boson decays are typically isolated from the rest of the event activity, in contrast to background from misidentified taus, which are typically immersed in considerable hadronic activity. For each lepton candidate (e , μ , or τ_h), a cone is constructed around the lepton direction at the event vertex. An isolation variable is constructed from the scalar sum of the transverse energy of all reconstructed particles contained within the cone, excluding the contribution from the lepton candidate itself.

In 2011 (2012), an average of 10 (20) proton-proton interactions occurred per LHC bunch crossing, making the assignment of the vertex of the hard-scattering process non-trivial. For each reconstructed collision vertex, the sum of the p_T^2 of all tracks associated to the vertex is computed. The vertex for which this quantity is the largest is assumed to correspond to the hard-scattering process, and is referred to as the primary vertex. A correction is applied to the isolation variable to account for effects of additional interactions. For charged particles, only those associated with the primary vertex are considered in the isolation variable. For neutral particles, a correction is applied by subtracting the energy deposited in the isolation cone by charged particles not associated with the primary vertex, multiplied by a factor of 0.5. This factor corresponds approximately to the ratio of neutral to charged hadron production in the hadronization process of pile-up interactions. An η , p_T , and lepton-flavor dependent threshold on the isolation variable of less than roughly 10% of the candidate p_T is applied.

To correct for the contribution to the jet energy due to pile-up, a median energy density (ρ) is determined event by event. The pile-up contribution to the jet energy is estimated as the product of ρ and the area of the jet and subsequently subtracted from the jet transverse energy [29]. In the fiducial region for jets of $|\eta| < 5.0$, jet energy corrections are also applied as a function of the jet E_T and η [30].

For taus decaying hadronically, the isolation variable is calculated using a multivariate *Boosted Decision Tree* (BDT) technique based on the neighboring reconstructed particles. Rings of radius $\Delta R = \sqrt{\Delta\phi^2 + \Delta\eta^2}$ are formed in the vicinity of the identified τ_h candidate and the moments of the energy deposits in η and ϕ and the energy density ρ in the event are used to define the isolation variable.

In this analysis, due to the small mass of the tau and its large p_T , the neutrinos produced in the tau decay tend to be produced nearly collinear with the visible products. Conversely, in $W + \text{jets}$ events, one of the main backgrounds, the high mass of the W results in a neutrino approximately opposite to the lepton in the transverse plane, while a jet is misidentified as a tau. In the $e\tau_h + X$ and $\mu\tau_h + X$ channel we therefore require the transverse mass

$$m_T = \sqrt{2p_T E_T^{\text{miss}} (1 - \cos(\Delta\phi))} \quad (1)$$

to be less than 40 GeV , where p_T is the lepton transverse momentum, and $\Delta\phi$ is the difference in ϕ of the lepton and E_T^{miss} vector.

In the $e\mu + X$ and the $\mu\mu + X$ search channel, we use a discriminator formed by considering the bisector of the directions of the visible tau decay products transverse to the beam direction,

denoted as the ζ axis [31]. From the projections of the visible decay product momenta and the E_T^{miss} vector onto the ζ axis, two values are calculated:

$$P_\zeta = p_{T,1} \cdot \zeta + p_{T,2} \cdot \zeta + E_T^{\text{miss}} \cdot \zeta, \quad (2)$$

$$P_\zeta^{\text{vis}} = p_{T,1} \cdot \zeta + p_{T,2} \cdot \zeta, \quad (3)$$

where the indices $p_{T,1}$ and $p_{T,2}$ indicate the transverse momentum of two reconstructed leptons. For the $e\mu+X$ and $\mu\mu+X$ channel we require $P_\zeta - 0.85 \cdot P_\zeta^{\text{vis}} > -25 \text{ GeV}$.

To further enhance the sensitivity of the search for Higgs bosons, we split the sample of selected events into five mutually exclusive categories based on the jet multiplicity, and the transverse momentum of the visible tau decay.

The event categories are:

- **VBF:** This event category is intended to exploit the production of Higgs bosons via vector-boson fusion (VBF). In this category two selected jets with $p_T > 30 \text{ GeV}$ are required. The events are characterized by a multivariate BDT discriminator, based on the invariant mass of the two jets, the differences $\Delta\eta(jj)$ ($\Delta\phi(jj)$) in η (ϕ) between the two jets, the p_T of the di- τ system including missing transverse energy, the p_T of the di-jet system, the difference in η between the visible part of the di- τ system and the closest jet and the visible p_T of the di- τ system. This discriminator is required to be larger than 0.5. To suppress background from $t\bar{t}$ events in the $e\mu+X$ channel an additional veto on any additional b -tagged jet with $p_T > 20 \text{ GeV}$ is applied. We require that there are no reconstructed jets with $p_T > 30 \text{ GeV}$ in the rapidity gap between the two tagging jets.
- **Boosted:** This event category is intended to exploit the production of a high- p_T Higgs boson, recoiling against a high- p_T jet. The p_T of the Higgs boson leads to a selection of events with higher E_T^{miss} in the hard scattering process which, due to the better precision of the E_T^{miss} measurement, improves the reconstruction of the invariant di- τ mass. In addition it allows to distinguish the Higgs boson signal from the irreducible background from Drell-Yan production of di- τ pairs, which is expected to have a softer p_T spectrum. In this category at least one jet with $p_T > 30 \text{ GeV}$ is required. The event is required not to be part of the VBF event category and a veto is applied on the presence of b -tagged jets with $p_T > 20 \text{ GeV}$ to suppress $t\bar{t}$ background.
- **0-Jet:** All selected events that are not part of any other event category described above is collected in this event category. It contains events without jets with $p_T > 30 \text{ GeV}$ and, in the $e\mu+X$ and $\mu\mu+X$ channel, without b -tagged jet with $p_T > 20 \text{ GeV}$.

The Boosted and 0-Jet categories are split in two bins of reconstructed transverse momentum. For the $e\tau_h+X$ and $\mu\tau_h+X$ channel the threshold is at $p_T > 40 \text{ GeV}$ of the hadronic tau, while the threshold is 35 GeV on the muon in the $e\mu+X$ channel and 20 GeV on the leading muon in the $\mu\mu+X$ channel.

The observed number of events for each category, as well as the expected number of events from various background processes, are shown in Tables 1–4 together with expected signal yields and efficiencies. The largest source of events selected with these requirements is $Z \rightarrow \tau\tau$ decays. We estimate the contribution from this process using an observed sample of $Z \rightarrow \mu\mu$ events, where the reconstructed muons are replaced by the reconstructed particles from simulated tau decays, a procedure called *embedding*. The normalization for this process is determined from the measurement of the $Z \rightarrow \mu\mu$ yield in data.

Another significant source of background is multijet events in which there is one jet misidentified as an isolated electron or muon, and a second jet misidentified as τ_h . $W+jets$ events in which there is a jet misidentified as a τ_h are also a source of background. The rates for these processes are estimated using the number of observed same-charge tau pair events, and from events with large transverse mass, respectively. Other background processes include $t\bar{t}$ production and $Z \rightarrow ee/\mu\mu$ events, particularly in the $e\tau_h+X$ channel due to the 2–3% probability for electrons to be misidentified as τ_h [28]. The small background from $W+jets$ and multijet events for the $e\mu+X$ channel where jets are misidentified as isolated leptons is derived by measuring the number of events with one good lepton and a second one which passes relaxed selection criteria, but fails the nominal lepton selection. This sample is extrapolated to the signal region using the efficiencies for such loose lepton candidates to pass the nominal lepton selection. These efficiencies are measured in data using multijet events. Backgrounds from $t\bar{t}$ and di-boson production are estimated from simulation using the MADGRAPH [32] event generator to simulate the shapes for $t\bar{t}$ events, and PYTHIA 6.424 [33] to simulate the shapes for di-boson events. The event yields are determined from measurements in background-enriched sideband regions.

To model the SM Higgs boson signals the event generators PYTHIA and POWHEG [34] are used. The TAUOLA [35] package is used for tau decays in all cases. Additional next-to-next-to-leading order (NNLO) K-factors from FEHICPRO [36, 37] are applied to the Higgs boson p_T spectrum from Higgs boson events produced via gluon fusion for samples produced at $\sqrt{s} = 7$ TeV. Samples produced at $\sqrt{s} = 8$ TeV use an improved version of POWHEG which shows good agreement in the Higgs boson p_T spectrum at NNLO.

The presence of pile-up is incorporated by simulating additional interactions and then reweighting the simulated events to match the distribution of additional interactions observed in data. The events in the embedded $Z \rightarrow \tau\tau$ sample and in other background samples obtained from data contain the correct distribution of pile-up interactions. The missing transverse energy response from simulation is corrected using a prescription, based on data, developed for inclusive W and Z cross section measurements [38], where Z bosons are reconstructed in the dimuon channel, and the missing transverse energy scale and resolution calibrated as a function of the Z boson transverse momentum.

3 Tau-pair invariant mass reconstruction

To distinguish the Higgs boson signal from the background, we reconstruct the tau-pair mass $m_{\tau\tau}$ using a maximum likelihood technique [39]. The algorithm computes the tau-pair mass that is most compatible with the observed momenta of visible tau decay products and the missing transverse energy reconstructed in the event. Free parameters, corresponding to the missing neutrino momenta, are subject to kinematic constraints and are eliminated by marginalization. The algorithm yields a tau-pair mass distribution consistent with the true value and a width of 15–20%.

4 Systematic uncertainties

Various imperfectly known or simulated effects can alter the shape and normalization of the invariant mass spectrum. The main contributions to the normalization uncertainty include the uncertainty in the total integrated luminosity (4.5%) [40], jet energy scale (2–5% depending on η and p_T), background normalization (Tables 1– 4), Z boson production cross section (2.5%) [38], lepton identification and isolation efficiency (1.0%), and trigger efficiency (1.0%).

Table 1: Numbers of expected and observed events in the event categories for the data taken in 2011 and 2012 as described in the text for the $e\tau_h+X$ channel. Categories of high and low tau pT are summed. Also given are the expected signal yields and the reconstruction and selection efficiency for a SM Higgs boson with $m_H = 125$ GeV in the various considered production channels. Combined statistical and systematic uncertainties on each estimate are reported.

Process	0-Jet	Boosted	VBF
$Z \rightarrow \tau\tau$	2552 ± 115	2130 ± 105	53 ± 5
QCD	909 ± 67	414 ± 26	35 ± 7
W+jets	1210 ± 72	1111 ± 73	46 ± 10
$Z+jets$ (l/jet faking τ)	558 ± 82	193 ± 21	13 ± 2
$t\bar{t}$	161 ± 15	108 ± 8	7.0 ± 1.7
Dibosons	19 ± 3	60 ± 9	1.2 ± 0.9
Total Background	5411 ± 168	4017 ± 133	156 ± 13
$H \rightarrow \tau\tau$	15 ± 1	25 ± 1	4.3 ± 0.6
Data	5273	3972	142

Signal Eff.

$gg \rightarrow H$	$1.3 \cdot 10^{-3}$	$1.2 \cdot 10^{-3}$	$8.0 \cdot 10^{-4}$
$qq \rightarrow qqH$	$3.8 \cdot 10^{-5}$	$2.1 \cdot 10^{-4}$	$5.2 \cdot 10^{-4}$
$qq \rightarrow Ht\bar{t}$ or VH	$1.3 \cdot 10^{-3}$	$1.9 \cdot 10^{-3}$	$1.8 \cdot 10^{-3}$

Table 2: Numbers of expected and observed events in the event categories for the data taken in 2011 and 2012 as described in the text for the $\mu\tau_h+X$ channel. Categories of high and low tau pT are summed. Also given are the expected signal yields and the reconstruction and selection efficiency for a SM Higgs boson with $m_H = 125$ GeV in the various considered production channels. Combined statistical and systematic uncertainties on each estimate are reported.

Process	0-Jet	Boosted	VBF
$Z \rightarrow \tau\tau$	50480 ± 2517	10568 ± 510	100 ± 9
QCD	14147 ± 2229	3979 ± 507	41 ± 9
W+jets	13256 ± 1180	5603 ± 468	72 ± 15
$Z+jets$ (l/jet faking τ)	1617 ± 245	659 ± 126	2.5 ± 0.6
$t\bar{t}$	651 ± 58	479 ± 40	14 ± 3
Dibosons	297 ± 47	256 ± 40	2.9 ± 2.1
Total Background	80448 ± 3569	21544 ± 865	233 ± 20
$H \rightarrow \tau\tau$	138 ± 9	84 ± 5	7.7 ± 1.1
Data	80229	22009	263

Signal Eff.

$gg \rightarrow H$	$1.4 \cdot 10^{-2}$	$3.5 \cdot 10^{-3}$	$3.2 \cdot 10^{-3}$
$qq \rightarrow qqH$	$1.9 \cdot 10^{-4}$	$6.1 \cdot 10^{-4}$	$1.2 \cdot 10^{-3}$
$qq \rightarrow Ht\bar{t}$ or VH	$3.9 \cdot 10^{-3}$	$3.5 \cdot 10^{-3}$	$4.2 \cdot 10^{-3}$

Table 3: Numbers of expected and observed events in the event categories for the data taken in 2011 and 2012 as described in the text for the $e\mu+X$ channel. Categories of high and low tau p_T are summed. Also given are the expected signal yields and the reconstruction and selection efficiency for a SM Higgs boson with $m_H = 125$ GeV in the various considered production channels. Combined statistical and systematic uncertainties on each estimate are reported.

Process	0-Jet	Boosted	VBF
$Z \rightarrow \tau\tau$	22029 ± 4285	5026 ± 907	56 ± 12
QCD	936 ± 97	551 ± 92	7.4 ± 1.4
$t\bar{t}$	39 ± 1	832 ± 29	24 ± 2
Dibosons	795 ± 45	549 ± 40	11 ± 2
Total Background	23799 ± 4285	6958 ± 913	99 ± 13
$H \rightarrow \tau\tau$	51 ± 2	33 ± 2	3.5 ± 0.4
Data	23274	6847	110

Signal Eff.

$gg \rightarrow H$	$5.4 \cdot 10^{-3}$	$1.6 \cdot 10^{-3}$	$7.8 \cdot 10^{-4}$
$qq \rightarrow qqH$	$5.5 \cdot 10^{-5}$	$3.1 \cdot 10^{-4}$	$3.8 \cdot 10^{-4}$
$qq \rightarrow Ht\bar{t}$ or VH	$1.0 \cdot 10^{-3}$	$3.9 \cdot 10^{-3}$	$2.1 \cdot 10^{-3}$

Table 4: Numbers of expected and observed events in the event categories for the data taken in 2011 and 2012 as described in the text for the $\mu\mu+X$ channel. Categories of high and low tau p_T are summed. Also given are the expected signal yields and the reconstruction and selection efficiency for a SM Higgs boson with $m_H = 125$ GeV in the various considered production channels. Combined statistical and systematic uncertainties on each estimate are reported.

Process	0-Jet	Boosted	VBF
$Z \rightarrow \tau\tau$	9117 ± 306	1985 ± 90	5.3 ± 0.4
QCD	759 ± 52	341 ± 26	0.0 ± 0.0
W+jets	145 ± 8	19 ± 1	0.0 ± 0.0
$Z \rightarrow \mu\mu$	1262911 ± 63251	379708 ± 21238	70 ± 8
$t\bar{t}$	2443 ± 180	1331 ± 120	6.7 ± 1.5
Dibosons	1502 ± 1063	2205 ± 787	2.4 ± 0.9
Total Background	1276877 ± 63261	385590 ± 21253	85 ± 9
$H \rightarrow \tau\tau$	24 ± 1	16 ± 1	0.8 ± 0.1
Data	1291874	385494	83

Signal Eff.

$gg \rightarrow H$	$4.8 \cdot 10^{-3}$	$3.4 \cdot 10^{-4}$	$2.0 \cdot 10^{-3}$
$qq \rightarrow qqH$	$7.6 \cdot 10^{-5}$	$5.3 \cdot 10^{-5}$	$5.5 \cdot 10^{-4}$
$qq \rightarrow Ht\bar{t}$ or VH	$5.6 \cdot 10^{-3}$	$4.6 \cdot 10^{-4}$	$7.7 \cdot 10^{-3}$

The tau-identification efficiency uncertainty is estimated to be 7% from an independent study done using a tag-and-probe technique [38] including the uncertainty of the trigger efficiency. The lepton identification and isolation efficiencies are stable as a function of the number of additional interactions in the bunch crossing in data and in Monte Carlo simulation. The b -tagging efficiency carries an uncertainty of 10%, and the b -mistag rate is accurate to 30% [41]. Uncertainties that contribute to mass spectrum shape variations include the tau (3%), muon (1%), and electron (1.5%) energy scales. The effect of the uncertainty on the E_T^{miss} scale, mainly due to pile-up effects, is incorporated by varying the mass spectrum shape as described in the next section.

The various production cross sections and branching fractions for SM and corresponding uncertainties are taken from [42–66]. Theoretical uncertainties on the Higgs production cross section are included in the search. These uncertainties are 12% for gluon fusion and 10% for VBF production.

5 Maximum likelihood fit

To search for the presence of a Higgs boson signal in the selected events, we perform a binned maximum likelihood fit to the tau-pair invariant-mass spectrum. The fit is performed jointly across four final states with five event categories each.

Systematic uncertainties are represented by nuisance parameters in the fitting process. We assume log-normal priors for normalization parameters, and Gaussian priors for mass-spectrum shape uncertainties. The uncertainties that affect the shape of the mass spectrum, mainly those corresponding to the energy scales, are represented by nuisance parameters whose variation results in a continuous perturbation of the spectrum shape [67].

6 Results

Figures 1 to 4 show the distributions of $m_{\tau\tau}$ for each event category compared with the background prediction. The categories of different tau- p_T are summed. The background mass distributions show the results of the fit using the background-only hypothesis.

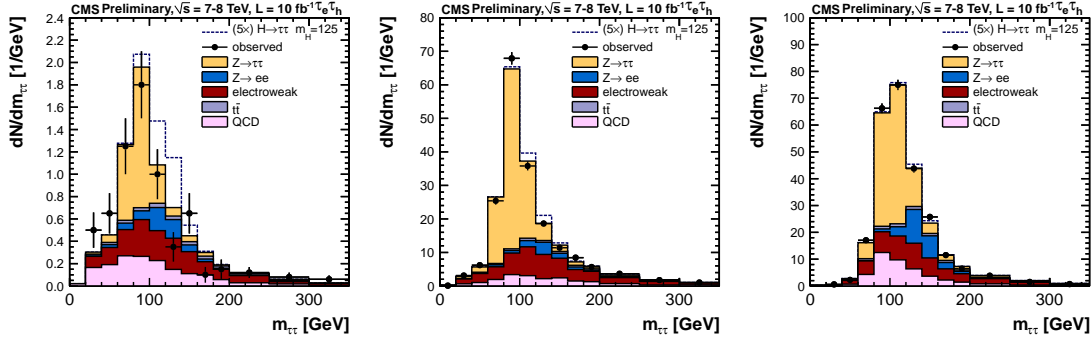


Figure 1: Distribution of the tau-pair invariant mass for the $\text{et}_h + X$ channel in the SM Higgs boson search categories: VBF category (left), Boosted category (middle), and 0-Jet category (right). The background labelled ‘electroweak’ combines the contribution from $W + \text{jets}$, $Z \rightarrow ll$, and diboson processes.

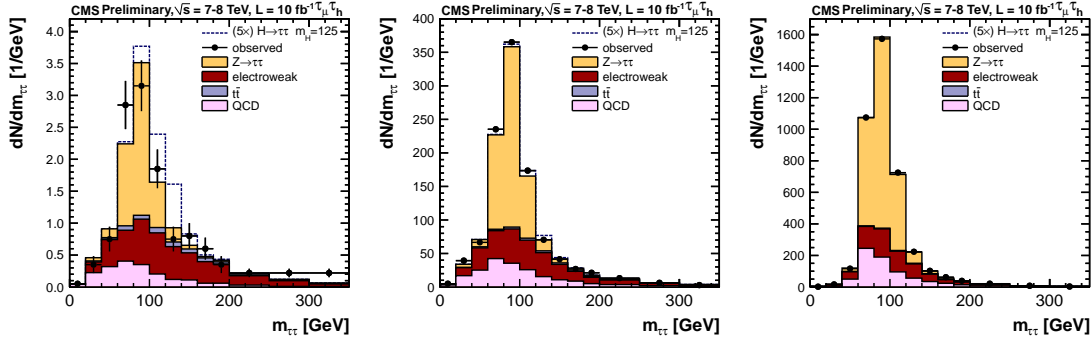


Figure 2: Distribution of the tau-pair invariant mass for the $\mu\tau_h + X$ channel in the SM Higgs boson search categories: VBF category (left), Boosted category (middle), and 0-Jet category (right). The background labelled ‘electroweak’ combines the contribution from $W + \text{jets}$, $Z \rightarrow ll$, and diboson processes.

The invariant mass spectra show no evidence for the presence of a Higgs boson signal, and we therefore set 95% confidence level (CL) upper bounds on the Higgs boson cross section times the branching fraction into a tau pair. For calculations of exclusion limits, we use the modified frequentist construction CL_s [68–70]. Theoretical uncertainties on the Higgs boson production cross sections are taken into account as systematic uncertainties in the limit calculations.

6.1 Limits on SM Higgs boson production

The 0-jet, Boosted, and VBF categories are used to set a 95% CL upper limit on the product of the Higgs boson production cross section and the $H \rightarrow \tau\tau$ branching fraction, $\sigma_H \times \text{BR}(H \rightarrow \tau\tau)$, with respect to the SM Higgs expectation, $\sigma/\sigma_{\text{SM}}$. Figure 5 shows the observed and the mean expected 95% CL upper limits for Higgs boson mass hypotheses ranging from 110 to 145 GeV. The bands represent the one- and two-standard-deviation probability intervals around the ex-

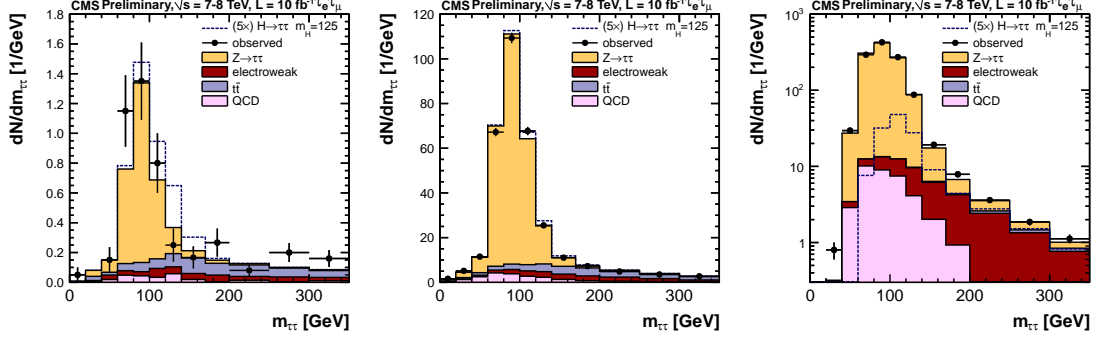


Figure 3: Distribution of the tau-pair invariant mass for the $e\mu+X$ channel in the SM Higgs boson search categories: VBF category (left), Boosted category (middle), and 0-Jet category (right).

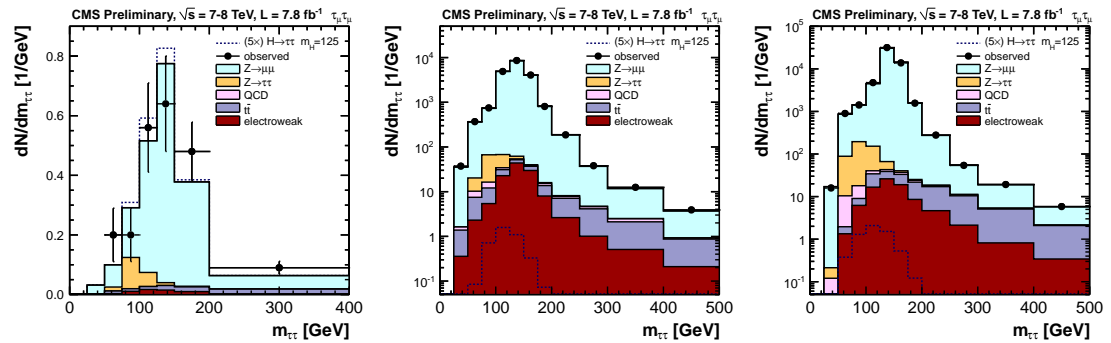


Figure 4: Distribution of the tau-pair invariant mass for the $\mu\mu+X$ channel in the SM Higgs boson search categories: VBF category (left), Boosted category (middle), and 0-Jet category (right).

pected limit. Table 5 shows the results for selected mass values. We set a 95% upper limit on $\sigma/\sigma_{\text{SM}}$ in the range of 1.06–3.36.

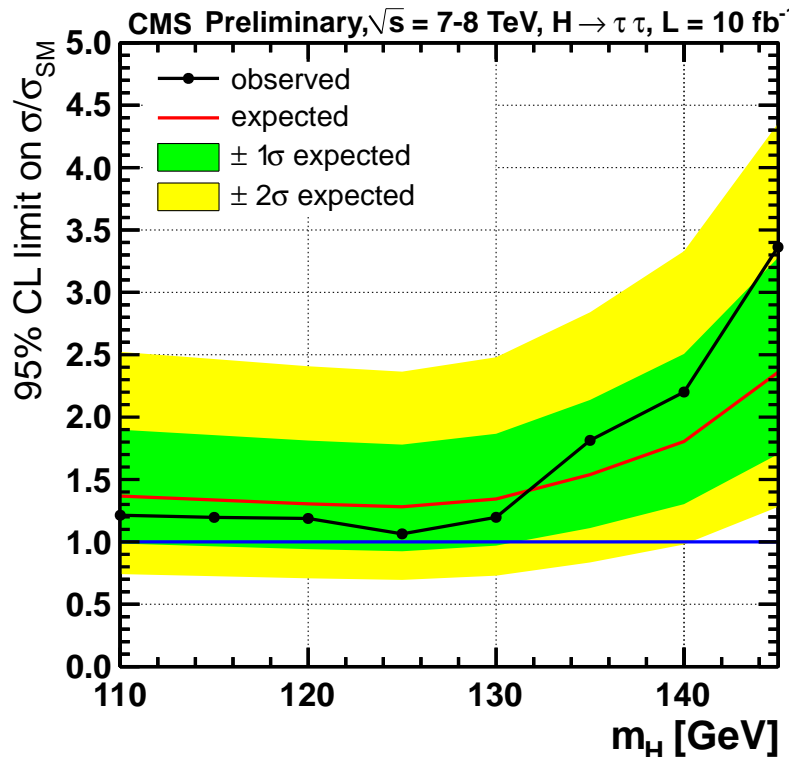


Figure 5: The expected one- and two-standard-deviation ranges are shown together with the observed 95% CL upper limits on the cross section, normalized to the SM expectation for Higgs boson production, as a function of m_H .

6.2 Comparison with previous results

In comparison with the results reported in [71], the sensitivity of the search has been improved significantly. The sensitivity of the search was increased by dividing the di-tau events into classes according to indicators of mass resolution and signal-to-background ratio, and combining the result in each category. The visible tau transverse momentum is used in the improved analysis together with the jet multiplicity already used in the previous result. The di-tau mass reconstruction has been improved with a more complete description of the likelihood and achieves a 25% better resolution. Furthermore, the identification of the basic objects, electron, muons, tau, jets and missing transverse energy has been optimized. Despite the increased level of pile-up in 2012, the analysis was able to maintain its performance through an improved jet identification which allows the rejection of jets with a low likelihood to stem from the hard interaction.

7 Summary

We have reported a search for SM Higgs boson, using a sample of CMS data from proton-proton collisions at a center-of-mass energy of 7 and 8 TeV at the LHC, corresponding to an integrated luminosity of 10 fb^{-1} . The tau-pair decay mode in final states with one e or μ plus a hadronic decay of a tau, the $e\mu$, and the $\mu\mu$ final state are used. The observed tau-pair mass

Table 5: Expected range and observed 95% CL upper limits on the cross section, divided by the expected SM Higgs cross section as a function of m_H .

SM Higgs	Expected limit					Obs. limit
	-2σ	-1σ	Median	$+1\sigma$	$+2\sigma$	
m_H [GeV]	-2σ	-1σ	Median	$+1\sigma$	$+2\sigma$	Obs. limit
110	0.742	0.987	1.37	1.9	2.52	1.21
115	0.725	0.964	1.34	1.86	2.47	1.20
120	0.708	0.942	1.3	1.81	2.41	1.19
125	0.695	0.925	1.28	1.78	2.36	1.06
130	0.729	0.97	1.34	1.87	2.48	1.20
135	0.835	1.11	1.54	2.14	2.84	1.81
140	0.979	1.3	1.8	2.51	3.33	2.20
145	1.28	1.7	2.36	3.28	4.35	3.36

spectra reveal no evidence for Higgs boson production. We determine a 95% CL upper limit in the mass range of 110–145 GeV on the Higgs boson production cross section. We exclude a Higgs boson with $m_H = 125$ GeV with a production cross section 1.06 times of that predicted by the standard model.

References

- [1] S. L. Glashow, “Partial Symmetries of Weak Interactions”, *Nucl. Phys.* **22** (1961) 579, doi:10.1016/0029-5582(61)90469-2.
- [2] S. Weinberg, “A Model of Leptons”, *Phys. Rev. Lett.* **19** (1967) 1264, doi:10.1103/PhysRevLett.19.1264.
- [3] A. Salam, “Weak and electromagnetic interactions”, in *Elementary particle physics: relativistic groups and analyticity*, N. Svartholm, ed., p. 367. Almqvist & Wiksell, Stockholm, 1968. Proceedings of the eighth Nobel symposium.
- [4] F. Englert and R. Brout, “Broken symmetry and the mass of gauge vector mesons”, *Phys. Rev. Lett.* **13** (1964) 321, doi:10.1103/PhysRevLett.13.321.
- [5] P. W. Higgs, “Broken symmetries, massless particles and gauge fields”, *Phys. Lett.* **12** (1964) 132, doi:10.1016/0031-9163(64)91136-9.
- [6] P. W. Higgs, “Broken symmetries and the masses of gauge bosons”, *Phys. Rev. Lett.* **13** (1964) 508, doi:10.1103/PhysRevLett.13.508.
- [7] G. S. Guralnik, C. R. Hagen, and T. W. B. Kibble, “Global conservation laws and massless particles”, *Phys. Rev. Lett.* **13** (1964) 585, doi:10.1103/PhysRevLett.13.585.
- [8] P. W. Higgs, “Spontaneous symmetry breakdown without massless bosons”, *Phys. Rev.* **145** (1966) 1156, doi:10.1103/PhysRev.145.1156.
- [9] T. W. B. Kibble, “Symmetry breaking in non-Abelian gauge theories”, *Phys. Rev.* **155** (1967) 1554, doi:10.1103/PhysRev.155.1554.
- [10] ALEPH, DELPHI, L3, OPAL Collaborations, and the LEP Working Group for Higgs Boson Searches Collaboration, “Search for the standard model Higgs boson at LEP”, *Phys. Lett. B* **565** (2003) 61, doi:10.1016/S0370-2693(03)00614-2, arXiv:hep-ex/0306033.

[11] CDF and D0 Collaboration, “Combination of Tevatron Searches for the standard model Higgs Boson in the W^+W^- Decay Mode”, *Phys. Rev. Lett.* **104** (2010) 061802, doi:10.1103/PhysRevLett.104.061802. A more recent, unpublished, limit is given in preprint arXiv:1103.3233.

[12] ATLAS Collaboration, “Combined search for the Standard Model Higgs boson in pp collisions at $\sqrt{s} = 7$ TeV with the ATLAS detector”, arXiv:1207.0319. Submitted to *Phys. Rev. D*.

[13] CMS Collaboration, “Combined results of searches for the standard model Higgs boson in pp collisions at $\sqrt{s} = 7$ TeV”, *Phys. Lett. B* **710** (2012) 26, doi:10.1016/j.physletb.2012.02.064.

[14] CMS Collaboration, “Combination of SM, SM4, FP Higgs boson searches”, CMS Physics Analysis Summary CMS-PAS-HIG-12-008, (2012).

[15] ALEPH, CDF, D0, DELPHI, L3, OPAL, SLD Collaborations, the LEP Working Group, the Tevatron Electroweak Working Group, and the SLD Electroweak and Heavy flavor Group, “Precision electroweak measurements and constraints on the standard model”, (2010). arXiv:hep-ex/1012.2367.

[16] CMS Collaboration, “The CMS experiment at the CERN LHC”, *JINST* **3** (2008) S08004, doi:10.1088/1748-0221/3/08/S08004.

[17] H. Georgi, S. Glashow, M. Machacek et al., “Higgs Bosons from Two Gluon Annihilation in Proton Proton Collisions”, *Phys. Rev. Lett.* **40** (1978) 692, doi:10.1103/PhysRevLett.40.692.

[18] D. L. Rainwater, D. Zeppenfeld, and K. Hagiwara, “Searching for $H \rightarrow \tau\tau$ in weak boson fusion at the CERN LHC”, *Phys. Rev. D* **59** (1998) 014037, doi:10.1103/PhysRevD.59.014037, arXiv:hep-ph/9808468.

[19] R. N. Cahn, S. D. Ellis, R. Kleiss et al., “Transverse Momentum Signatures for Heavy Higgs Bosons”, *Phys. Rev. D* **35** (1987) 1626, doi:10.1103/PhysRevD.35.1626.

[20] CMS Collaboration, “Electron Reconstruction and Identification at $\sqrt{s} = 7$ TeV”, CMS Physics Analysis Summary CMS-PAS-EGM-10-004, (2010).

[21] CMS Collaboration, “Performance of muon identification in pp collisions at $\sqrt{s} = 7$ TeV”, CMS Physics Analysis Summary CMS-PAS-MUO-10-002, (2010).

[22] CMS Collaboration, “Measurement of Inclusive Z Cross Section via Decays to Tau Pairs in pp Collisions at $\sqrt{s}=7$ TeV”, *JHEP* **8** (2011) 117, doi:10.1007/JHEP08(2011)117.

[23] CMS Collaboration, “Particle-Flow Event Reconstruction in CMS and Performance for Jets, Taus, and E_T^{miss} ”, CMS Physics Analysis Summary CMS-PAS-PFT-09-001, (2009).

[24] CMS Collaboration, “Commissioning of the Particle-Flow Reconstruction in Minimum-Bias and Jet Events from pp Collisions at 7 TeV”, CMS Physics Analysis Summary CMS-PAS-PFT-10-002, (2010).

[25] CMS Collaboration, “Commissioning of the particle-flow event reconstruction with leptons from J/Ψ and W decays at 7 TeV”, CMS Physics Analysis Summary CMS-PAS-PFT-10-003, (2010).

- [26] M. Cacciari, G. P. Salam, and G. Soyez, “FastJet user manual”, arXiv:hep-ph/1111.6097v1.
- [27] M. Cacciari and G. P. Salam, “Dispelling the N^3 myth for the k_t jet-finder”, *Phys. Lett. B* **641** (2006) 57, doi:10.1016/j.physletb.2006.08.037, arXiv:hep-ph/0512210.
- [28] CMS Collaboration, “Performance of tau-lepton reconstruction and identification in CMS”, *JINST* **7** (2012) P01001, doi:10.1088/1748-0221/7/01/P01001.
- [29] M. Cacciari and G. P. Salam, “Pileup subtraction using jet areas”, *Phys. Lett. B* **659** (2008) 119, doi:10.1016/j.physletb.2007.09.077, arXiv:hep-ph/0707.1378.
- [30] CMS Collaboration, “Determination of Jet Energy Calibration and Transverse Momentum Resolution in CMS”, *JINST* **6** (2011) 11002, doi:10.1088/1748-0221/6/11/P11002.
- [31] C. C. Almenar, “Search for the neutral MSSM Higgs bosons in the $\tau\tau$ decay channels at CDF Run II”. PhD thesis, Universitat de València. FERMILAB-THESIS-2008-86. doi:10.2172/953708.
- [32] J. Alwall et al., “MadGraph/MadEvent v4: the new web generation”, *JHEP* **09** (2007) 028, doi:10.1088/1126-6708/2007/09/028, arXiv:hep-ph/0706.2334.
- [33] T. Sjöstrand, S. Mrenna, and P. Skands, “PYTHIA 6.4 physics and manual”, *JHEP* **05** (2006) 026, doi:10.1088/1126-6708/2006/05/026.
- [34] S. Frixione, P. Nason, C. Oleari, “Matching NLO QCD computations with parton shower simulations: the POWHEG method”, *JHEP* **11** (2007) 070, doi:10.1088/1126-6708/2007/11/070.
- [35] Z. Wąs, “TAUOLA the library for tau lepton decay, and KKMC/KORALB/KORALZ...status report”, *Nucl. Phys. B, Proc. Suppl.* **98** (2001) 96, doi:10.1016/S0920-5632(01)01200-2.
- [36] C. Anastasiou, K. Melnikov, and F. Petriello, “Fully differential Higgs boson production and the di-photon signal through next-to-next-to-leading order”, *Nucl. Phys. B* **724** (2005) 197, doi:10.1016/j.nuclphysb.2005.06.036.
- [37] C. Anastasiou, S. Bucherer, and Z. Kunszt, “HPro: A NLO Monte-Carlo for Higgs production via gluon fusion with finite heavy quark masses”, *JHEP* **10** (2009) 068, doi:10.1088/1126-6708/2009/10/068.
- [38] CMS Collaboration, “Measurement of Inclusive W and Z Cross Sections in pp Collisions $\sqrt{s}=7$ TeV”, *JHEP* **1110** (2011) 132, doi:10.1007/JHEP01(2011)080.
- [39] CMS Collaboration, “Search for neutral MSSM Higgs bosons decaying to tau pairs in pp collisions at $\sqrt{s} = 7$ TeV”, *Phys. Rev. Lett.* **106** (2011) 231801, doi:10.1103/PhysRevLett.106.231801.
- [40] CMS Collaboration, “Measurement of CMS Luminosity”, CMS Physics Analysis Summary CMS-PAS-EWK-10-004, (2010).
- [41] CMS Collaboration, “Performance of b-jet identification in CMS”, CMS Physics Analysis Summary CMS-PAS-BTV-11-001, (2011).

[42] LHC Higgs Cross Section Working Group, “Handbook of LHC Higgs Cross Sections: 1. Inclusive Observables”, CERN Report CERN-2011-002, (2011).

[43] A. Djouadi, M. Spira, and P. M. Zerwas, “Production of Higgs bosons in proton colliders: QCD corrections”, *Phys. Lett.* **B264** (1991) 440, doi:10.1016/0370-2693(91)90375-Z.

[44] S. Dawson, “Radiative corrections to Higgs boson production”, *Nucl. Phys. B* **359** (1991) 283, doi:10.1016/0550-3213(91)90061-2.

[45] M. Spira, A. Djouadi, D. Graudenz et al., “Higgs boson production at the LHC”, *Nucl. Phys. B* **453** (1995) 17, doi:10.1016/0550-3213(95)00379-7.

[46] R. V. Harlander and W. B. Kilgore, “Next-to-next-to-leading order Higgs production at hadron colliders”, *Phys. Rev. Lett.* **88** (2002) 201801, doi:10.1103/PhysRevLett.88.201801, arXiv:hep-ph/0201206.

[47] C. Anastasiou and M. Charalampou, “Higgs boson production at hadron colliders in NNLO QCD”, *Nucl. Phys. B* **646** (2002) 220, doi:10.1016/S0550-3213(02)00837-4, arXiv:hep-ph/0207004.

[48] V. Ravindran, J. Smith, and W. L. van Neerven, “NNLO corrections to the total cross section for Higgs boson production in hadron hadron collisions”, *Nucl. Phys. B* **665** (2003) 325, doi:10.1016/S0550-3213(03)00457-7, arXiv:hep-ph/0302135.

[49] S. Catani et al., “Soft-gluon resummation for Higgs boson production at hadron colliders”, (2003). arXiv:hep-ph/0306211.

[50] U. Aglietti, R. Bonciani, G. Degrassi et al., “Two-loop light fermion contribution to Higgs production and decays”, *Phys. Lett.* **B595** (2004) 432, doi:10.1016/j.physletb.2004.06.063, arXiv:hep-ph/0404071.

[51] G. Degrassi and F. Maltoni, “Two-loop electroweak corrections to Higgs production at hadron colliders”, *Phys. Lett.* **B600** (2004) 255, doi:10.1016/j.physletb.2004.09.008, arXiv:hep-ph/0407249.

[52] S. Actis et al., “NLO Electroweak Corrections to Higgs Boson Production at Hadron Colliders”, *Phys. Lett. B* **670** (2008) 12, doi:10.1016/j.physletb.2008.10.018, arXiv:hep-ph/0809.1301.

[53] C. Anastasiou, R. Boughezal, and F. Petriello, “Mixed QCD-electroweak corrections to Higgs boson production in gluon fusion”, *JHEP* **04** (2009) 003, doi:10.1088/1126-6708/2009/04/003, arXiv:hep-ph/0811.3458.

[54] D. de Florian and M. Grazzini, “Higgs production through gluon fusion: updated cross sections at the Tevatron and the LHC”, *Phys. Lett. B* **674** (2009) 291, doi:10.1016/j.physletb.2009.03.033, arXiv:hep-ph/0901.2427.

[55] J. Baglio and A. Djouadi, “Higgs production at the LHC”, *JHEP* **03** (2011) 055, doi:10.1007/JHEP03(2011)055, arXiv:1012.0530.

[56] M. Ciccolini, A. Denner, and S. Dittmaier, “Strong and electroweak corrections to the production of Higgs + 2-jets via weak interactions at the LHC”, *Phys. Rev. Lett.* **99** (2007) 161803, doi:10.1103/PhysRevLett.99.161803, arXiv:hep-ph/0707.0381.

[57] M. Ciccolini, A. Denner, and S. Dittmaier, “Electroweak and QCD corrections to Higgs production via vector-boson fusion at the LHC”, *Phys. Rev. D* **77** (2008) 013002, doi:10.1103/PhysRevD.77.013002, arXiv:hep-ph/0710.4749.

[58] K. Arnold et al., “VBFNLO: A parton level Monte Carlo for processes with electroweak bosons”, *Comput. Phys. Commun.* **180** (2009) 1661, doi:10.1016/j.cpc.2009.03.006, arXiv:hep-ph/0811.4559.

[59] O. Brein, A. Djouadi, R. Harlander, “NNLO QCD corrections to the Higgs-strahlung processes at hadron colliders”, *Phys. Lett. B* **579** (2004) 149, doi:10.1016/j.physletb.2003.10.112, arXiv:hep-ph/0307206.

[60] M. L. Ciccolini, S. Dittmaier, and M. Krämer, “Electroweak radiative corrections to associated WH and ZH production at hadron colliders”, *Phys. Rev. D* **68** (2003) 073003, doi:10.1103/PhysRevD.68.073003, arXiv:hep-ph/0306234.

[61] A. Djouadi, J. Kalinowski, M. Muhlleitner et al., “An update of the program HDECAY”, in *The Les Houches 2009 workshop on TeV colliders: The tools and Monte Carlo working group summary report*. 2010. arXiv:hep-ph/1003.1643.

[62] A. Denner, S. Heinemeyer, I. Puljak et al., “Standard Model Higgs-Boson Branching Ratios with Uncertainties”, *Eur. Phys. J. C* **71** (2011) 1753, doi:10.1140/epjc/s10052-011-1753-8, arXiv:hep-ph/1107.5909.

[63] M. Botje, J. Butterworth, A. Cooper-Sarkar et al., “The PDF4LHC Working Group Interim Recommendations”, arXiv:hep-ph/1101.0538.

[64] S. Alekhin, S. Alioli, R. D. Ball et al., “The PDF4LHC Working Group Interim Report”, arXiv:hep-ph/1101.0536.

[65] H.-L. Lai, M. Guzzi, J. Huston et al., “New parton distributions for collider physics”, *Phys. Rev. D* **82** (2010) 074024, doi:10.1103/PhysRevD.82.074024.

[66] NNPDF Collaboration, “Impact of Heavy Quark Masses on Parton Distributions and LHC Phenomenology”, arXiv:hep-ph/1101.1300.

[67] J. S. Conway, “Nuisance Parameters in Likelihoods for Multisource Spectra”, in *Proceedings of PHYSTAT 2011 Workshop on Statistical Issues Related to Discovery Claims in Search Experiments and Unfolding*, H. Propser and L. Lyons, eds., number CERN-2011-006, p. 115. CERN, 2011.

[68] T. Junk, “Confidence level computation for combining searches with small statistics”, *Nucl. Instrum. Meth. A* **434** (1999) 435, doi:10.1016/S0168-9002(99)00498-2.

[69] A. L. Read, “Modified frequentist analysis of search results (the CLs method)”, CERN Report CERN-OPEN-2000-005, (2000).

[70] ATLAS and CMS Collaborations, LHC Higgs Combination Group, “Procedure for the LHC Higgs boson search combination in Summer 2011”, ATL-PHYS-PUB/CMS NOTE 2011-11, 2011/005, (2011).

[71] CMS Collaboration, “Search for neutral Higgs bosons decaying to tau pairs in pp collisions at $\sqrt{s} = 7$ TeV”, *Phys. Lett. B* **713** (2012) 68, doi:10.1016/j.physletb.2012.05.028.